Journal of Invertebrate Pathology 183 (2021) 107622

Contents lists available at ScienceDirect

Journal of Invertebrate Pathology

journal homepage: www.elsevier.com/locate/jip

New gregarine species (Apicomplexa) from tunicates show an evolutionary history of host switching and suggest a problem with the systematics of *Lankesteria* and *Lecudina*

Davis Iritani [a], Jonathan C. Banks [b], Stephen C. Webb [b], Andrew Fidler [c], Takeo Horiguchi [d], Kevin C. Wakeman [e,*]

[a] *Graduate School of Science, Hokkaido University, North 10, West 8, Sapporo 060-0810, Japan*
[b] *Cawthron Institute, 98 Halifax Street East, Nelson 7010, New Zealand*
[c] *AquaGeneNZ Ltd., Nelson 7010, New Zealand*
[d] *Faculty of Science, Hokkaido University, North 10, West 8, Sapporo 060-0810, Japan*
[e] *Institute for the Advancement of Higher Education, Hokkaido University, Sapporo 060-0815, Japan*

ARTICLE INFO

Keywords:
Apicomplexa
Ascidiacea
Eugregarinorida
Evolution
Morphology
Systematics

ABSTRACT

Apicomplexa (sensu stricto) are a diverse group of obligate parasites to a variety of animal species. Gregarines have been the subject of particular interest due to their diversity, phylogenetically basal position, and more recently, their symbiotic relationships with their hosts. In the present study, four new species of marine eugregarines infecting ascidian hosts (*Lankesteria kaiteriteriensis* sp. nov., *L. dolabra* sp. nov., *L. savignyii* sp. nov., and *L. pollywoga* sp. nov.) were described using a combination of morphological and molecular data. Phylogenetic analysis using small subunit rDNA sequences suggested that gregarines that parasitize ascidians and polychaetes share a common origin as traditionally hypothesized by predecessors in the discipline. However, *Lankesteria* and *Lecudina* species did not form clades as expected, but were instead intermixed amongst each other and their respective type species in the phylogeny. These two major genera are therefore taxonomically problematic. We hypothesize that the continued addition of new species from polychaete and tunicate hosts as well as the construction of multigene phylogenies that include type-material will further dissolve the currently accepted distinction between *Lankesteria* and *Lecudina*. The species discovered and described in the current study add new phylogenetic and taxonomic data to the knowledge of marine gregarine parasitism in ascidian hosts.

1. Introduction

Apicomplexa (sensu stricto; synonymous with Sporozoa Leuckart 1879) are a widespread group of unicellular eukaryotes that parasitize animal hosts. There are over 6000 named apicomplexans classified in ~ 350 genera and select constituent members such as *Plasmodium*, *Toxoplasma*, and *Cryptosporidium* have attracted special attention due to their medical or veterinary impact. For example, there are still 219 million cases of malaria per year (World Health Organization 2018) and 30% of the global human population is chronically infected by *Toxoplasma* (Schlüter et al., 2014). Focused research of these apicomplexans, whose parasitism heavily impacts human life, has led to many advances in apicomplexan biology (e.g., Abrahamsen et al., 2004; Kim and Weiss, 2004; Wilson et al., 1996). These well studied taxa, however, represent only a portion of the mostly undescribed total apicomplexan diversity, estimated at over one million species (Adl et al., 2007, 2012, 2019).

Marine gregarines are an understudied group that are of interest due to their ubiquity, diversity, and early branching position in the apicomplexan phylogeny. They parasitize a wide range of taxonomically and geographically distinct hosts and have retained key plesiomorphic characters (e.g., monoxeny, conspicuous feeding stages, and parasitism via myzocytosis) that are important for understanding apicomplexan diversification (Leander, 2008; Rueckert et al., 2011; Sitnikova and Shirokaya, 2013; Wakeman and Leander, 2013). The effects of gregarine presence in invertebrate hosts are the subject of ongoing research; a recent study has suggested that gregarines encompass the entire spectrum of symbiotic relationships including mutualism with their hosts (Rueckert et al., 2019). Gregarine parasitism, however, has been

* Corresponding author.
E-mail address: wakeman.k@oia.hokudai.ac.jp (K.C. Wakeman).

https://doi.org/10.1016/j.jip.2021.107622
Received 3 March 2020; Received in revised form 13 May 2021; Accepted 18 May 2021
Available online 24 May 2021

associated with decreased fecundity (Zuk, 1987) as well as the obstruction of digestive tracts (Mita et al., 2012) which is where most gregarine infections occur. Ecologically, the characterization of microbial pathogens in ascidians is important especially considering the serious biosecurity threats posed by ascidians as prolific invaders of marine ecosystems (Lambert, 2007; McKindsey et al., 2007; Zhan et al., 2015). Unfortunately, the bulk of gregarine taxa remain wholly undiscovered or represented only as environmental sequences. Thus, a major task for gregarine biology is to further explore the uncharted diversity of gregarines and to better understand key character traits within a molecular phylogenetic framework.

Gregarines are broadly divided into four major groups: Archigregarinorida, Neogregarinorida, Eugregarinorida, and Cryptogregarinorida (Adl et al., 2019). This classification scheme is rooted in morphology (e.g., cortical microtubules, attachment apparatuses, and cell shape), life history, and molecular phylogenies built on small subunit ribosomal DNA (SSU rDNA) data (Leander, 2006; Rueckert et al., 2013; Schrével et al., 2016; Simdyanov et al., 2017; Wakeman and Leander, 2012). The study of marine gregarines is especially concerned with the conspicuous feeding stage of the gregarine life cycle, known as the trophozoite, due to its more reliable or recognizable presence inside a host in contrast to the other stages such as the oocysts which can be challenging to recover once expelled into the environment.

Eugregarinorida Léger 1900 represent the majority of marine gregarine taxa, most of which are classified within the poorly resolved family Lecudinidae Kamm 1922 (Levine, 1977). The two major genera in this family are *Lankesteria* Mingazzini 1891 (abbreviated *La.* herein) and *Lecudina* Mingazzini 1891 (abbreviated *Le.* herein). *Lankesteria* was a poorly defined genus that encompassed taxonomically dissimilar species including gregarines that infect ascidians, chaetognaths, turbellarians, and insects (Levine, 1977). Following the movement of the insect gregarines from *Lankesteria* and into *Ascocystis* by Grassé (1953), Ormières (1965) proposed *Lankesteria* be retained solely for the gregarines that parasitize urochordates. *Lecudina* Mingazzini 1891, on the other hand, is a genus consisting of about 40 species that parasitize a variety of polychaete hosts (Levine, 1976). Théodoridès (1967) hypothesized that *Lankesteria* and *Lecudina* share a common evolutionary origin, but later diverged into two genera that infect distinct hosts (i.e., ascidians and polychaetes). There are indeed morphological similarities between *Lankesteria* and *Lecudina* such as unsegmented intracellular development, an elongated morphology that ends anteriorly at a mucron, head-to-head syzygy (Levine, 1977), and overall lifecycle (Desportes and Schrével, 2013). Early molecular phylogenetic studies supported distinct *Lankesteria* and *Lecudina* lineages and revealed three subclades comprised of (1) *La. abbotti* and *La.* sp.; (2) *Le. tuzetae* and an environmental sequence; and (3) *La. chelysomae* and *La. cystodytae* (Desportes and Schrével, 2013). Desportes and Schrével (2013) elaborate that the above-mentioned subclades (1) and (3) not clustering together to form a clade is a situation which requires additional molecular data to address. Other recent studies on *Lankesteria* and *Lecudina* include species descriptions and phylogenetic analyses (e.g., Iritani et al., 2017; Leander et al., 2003; Rueckert et al., 2015, 2013, 2010; Simdyanov et al., 2017) as well a study on their pathogenic effects (e.g., Mita et al., 2012). The two genera are shown to form separate clades based on all of these phylogenies.

In this study, we describe four new species of marine lecudinids that infect solitary sea squirts (Ascidiacea Blainville 1824) from New Zealand. The addition of these four novel taxa corroborates Théodoridès's hypothesis that gregarine parasites of tunicates and polychaetes share a common origin (Théodoridès, 1967). However, our data confound the taxonomic boundary between the two genera and suggest that *Lankesteria* and *Lecudina* require emendation to reflect phylogeny. The new species described in this study represent the first record of marine gregarines that parasitize ascidians in New Zealand.

2. Material and methods

2.1. Host collection and gregarine trophozoite isolation

Ascidians were collected from three locations around the South Island of New Zealand between March 1st and March 14th of 2019. *Pyura* sp. (*Pyura* species complex) was collected from the underside of boulders exposed during low tide from Kaiteriteri Beach, Kaiteriteri, New Zealand (41°02′07.7″S 173°01′21.4″E). Both *Ciona savignyi* (Pacific vase sea squirt) and *Molgula complanata* (sea grape) were collected from fouled ropes that hung submerged along the docks in Nelson Marina, Nelson, New Zealand (41°15′37.1″S 173°16′53.0″E). *Asterocarpa humilis* (compass sea squirt) was similarly collected from a fouled rope in Waikawa Marina, Marlborough, New Zealand (41°16′02.8″S 174°02′18.4″E).

The ascidians were transported back to the laboratory and kept in containers filled with seawater, separated by sampling locality. Each ascidian was dissected within two days of collection. The procedure involved removing the tunic and extracting the digestive tract from the posterior end of the pharyngeal basket to the anus. The extracted digestive tract, from the start of the intestine to the anus, was submerged in seawater filtered at 0.45 μm and split down its length using fine forceps to expose the contents of the gut. Gregarine trophozoites were observed under an inverted light microscope and isolated individually using hand-drawn glass pipettes. The trophozoites from each individual host were then washed in seawater filtered at 0.45 μm to remove potential contamination from host tissue and other exogenous eukaryote DNA. Trophozoites were pooled together for subsequent use in light microscopy or scanning electron microscopy; single-cell isolations were prepared for DNA extraction and sequencing.

2.2. Light microscopy

The morphology of live trophozoites was observed with an Olympus BX51 (Olympus, Tokyo, Japan) paired to an Olympus DP73 camera. Light micrographs presented in the current manuscript are composites of multiple high magnification photos taken along the length of the entire cell subsequently stitched together using Panorama Stitcher Mini version 1.10 (Olga Kacher, Boltnev Studio). Micrographs were then refined with GIMP version 2.10.12 (GNU image manipulation program version; The GIMP Team). The overall shape and size of the trophozoites were used to inform species delimitation. Trophozoite shapes were based on the nomenclature suggested by Clopton (2004).

2.3. Scanning electron microscopy

Trophozoites were pooled in porous baskets (50 μm), separately for each individual host, and fixed with 2.5% glutaraldehyde for 30 mins on ice. The fixative was washed out with chilled, filtered seawater. Fixation continued with the addition of 1% OsO_4 and the trophozoites were left for 30 min on ice. The fixative was again removed with chilled, filtered seawater. The trophozoites were then dehydrated in a graded series of ethanol for three minutes at each of the following concentrations: 50%, 70%, 80%, 90%, and 100%. A Leica EM CPD300 (Leica Microsystems, Wetzlar, Germany) was used for critical point drying. Each SEM stub was sputter coated with gold for 180 s at 15 μA. Scanning electron micrographs were taken on a Hitachi S3000N scanning electron microscope and placed on a black background using GIMP version 2.10.

2.4. DNA extraction, amplification and sequencing

For each gregarine species, trophozoites were individually isolated, washed three times with filtered and autoclaved seawater, and placed in separate 0.2 ml PCR tubes. Genomic DNA was extracted from the single-cell isolates using a QuickExtract FFPE RNA Extraction Kit (Epicentre, Wisconsin, USA). The SSU rDNA sequences were initially amplified by a polymerase chain reaction (PCR) using universal eukaryote primers PF1

5′ – CGCTACCTGGTTGATCCTGCC – 3′ and SSUR4 5′ – GATCCTTCTGCAGGTTCACCTAC – 3′ (expected length: ~1800 bp; Leander et al., 2003) and TaKaRa Ex Taq (Takara Bio Inc., Otsu, Japan). The thermal cycler conditions used were as follows: initial denaturation at 94 °C for 1 min followed by 35 cycles of denaturation at 94 °C for 20 s, annealing at 56 °C for 30 s, extension at 72 °C for 1:40 min, and a final extension at 72 °C for 7 min. The product from this initial amplification was diluted 1:100 in distilled water and used as template for nested PCRs using the specific gregarine primer pairs developed for this study: T74F 5′ – GTCTCGCAGATTAAGCCATG – 3′ paired with T1140R 5′ – GAATACGAATGCCCTCAACC – 3′ (expected length: ~900 bp) and T990F 5′ – GAGTGAATCGGCGTGTTC – 3′ paired with T1791R 5′ - CTCCGCCTAACTCATGATAC – 3′ (expected length: ~900 bp). These nested PCRs served to further ensure that the final sequences recovered excluded contamination from exogenous eukaryotic DNA as well as to split the SSU rDNA into lengths appropriate for Sanger sequencing. The thermal cycler conditions used were as follows: initial denaturation at 94 °C for 1 min followed by 35 cycles of denaturation at 94 °C for 20 s, annealing at 52 °C for 30 s, extension at 72 °C for 1:40 min, and a final extension at 72 °C for 7 min. The products were purified with polyethylene glycol (PEG), prepared for sequencing with a BigDye® Terminator v1.1 Cycle Sequencing Kit (Applied Biosystems, Waltham, USA), and sequenced using the same internal primers used for the nested PCRs. The SSU rDNA sequences for each single-cell isolation were assembled on MEGA 7 (Kumar et al., 2016) by aligning the nested PCR amplicons and were initially identified using Basic Local Alignment and Search Tool (BLAST).

Identification of the hosts was based on morphology using a species guide (Page et al., 2019) and the top BLAST hit for each host using partial COI and SSU rDNA sequences amplified with Folmer primers (Folmer et al., 1994) or PF1 – 18SRF 5′ – CCCGTGTTGAGTCAAATTAAG – 3′ (Mo et al., 2002) and SR4 5′ – AGGGCAAGTCTGGTGCCAG – 3′ (Yamaguchi and Horiguchi, 2005) - SSUR4, respectively. The following thermal cycler conditions were used: initial denaturation at 94 °C for 1 min followed by 35 cycles of denaturation at 94 °C for 20 s, annealing at 47 °C or 50 °C for 30 s, extension at 72 °C for 0:40 s, and a final extension at 72 °C for 7 min.

2.5. Molecular phylogenetic analyses

A 90-taxon alignment of SSU rDNA sequences was analyzed, including three dinoflagellate sequences to form the outgroup and representative sequences from the major apicomplexan groups. Each gregarine species collected for this study was represented in the analysis as two to three separate sequences. Clades which are known to be situated on long phylogenetic branches (e.g., crustacean gregarines and *Trichotokara*) that had little relevance to the analysis of the ascidian gregarines were excluded from for the sake of clarity. The SSU rDNA sequences were aligned using MAFFT version 6 with the Q-INS-i option (Katoh et al., 2002) for its ability to account for the secondary structure of ribosomal subunits. Ambiguously aligned regions and gaps were cut from the final alignment using Aliscore version 2.0 (Kück et al., 2010; Misof and Misof, 2009) and Alicut version 2.31. The resulting alignment included 1440 unambiguously aligned nucleotides.

Maximum likelihood (ML) and Bayesian trees were constructed using RAxML version 8.2.12 (Stamatakis, 2014) and Mr. Bayes version 3.2.6 (Ronquist et al., 2012) through the Cipres Science Gateway version 3.3 (Miller et al., 2010). The GTR + I + Γ model was suggested by jModelTest version 2.1.10 (Darriba et al., 2012; Guindon and Gascuel, 2003) for phylogenetic analysis of the 90-taxon alignment (proportion of invariable sites = 0.1970, gamma shape = 0.6960). RAxML was run with default parameters, but with the GTRGAMMA + I parameter turned on. The parameters specified for Mr. Bayes were as follows: lset nst = 6, rates = invgamma, and Monte Carlo Markov Chains (MCMC) run for 10,000,000 generations (ngen = 10 000 000), 2 runs (nruns = 2), 4 chains (nchains = 4), temperature parameter at 0.2 (temp = 0.200), sample frequency of 100, prior burn-in of 25% of sampled trees, and a stop rule of 0.01 to terminate the program when the split deviation fell below 0.01.

3. Results

3.1. Lankesteria kaiteriteriensis sp. nov.

Cells were very narrowly to narrowly spatulate and arched to an overall crescent whereby a narrow posterior gently curved and widened markedly towards the middle of the cell, near the nucleus, and ended in a stubbed, and conspicuous mucron (Fig. 1A, B). Trophozoites were a dark, golden-brown near the periphery of the cell and at the posterior, which then transitioned to a more colourless brown and grey near the nucleus and ended at a mostly translucent mucron. The cells ranged between 165.3 and 405.7 μm ($\overline{X}$ = 268.0 μm, n = 80) in length and 32.7 to 114.6 μm ($\overline{X}$ = 50.0 μm, n = 80) in width at the widest point of the cell. An oval nucleus with a major axis between 38.5 and 71.7 μm ($\overline{X}$ = 56.3 μm, n = 20) and a minor axis between 35.7 and 66.0 μm ($\overline{X}$ = 49.6 μm, n = 20) was located in the anterior third of the cell. A distinct nucleolus with a ring-like appearance, measuring 14.8 to 31.6 μm ($\overline{X}$ = 25.4 μm, n = 20) by 17.2 to 29.7 μm ($\overline{X}$ = 23.7 μm, n = 80), was situated in the posterior half of the nucleus. The cell surface was comprised of epicytic folds arranged longitudinally at a density of 4 folds/μm (Fig. 1C). The mucron was observed to curl slightly inwards towards the center of the cell (Fig. 1D). Gliding motility was observed. Isolated from *Pyura* sp. Molina, 1782.

3.2. Lankesteria dolabra sp. nov.

General shape of the trophozoites was very narrowly spatulate consisting of a rod-like body and a tapering posterior which ended in a sharp point (Fig. 2A, B). The posterior ends of the cell and the mucron were translucent, but the rest of the cell was a light golden brown. The cells ranged between 163.7 and 207.1 μm ($\overline{X}$ = 173.7 μm, n = 40) in length and 22.7 to 43.5 μm ($\overline{X}$ = 32.6 μm, n = 40) in width at the widest point of the cell. The nucleus was inconspicuous with a major axis between 14.4 and 21.9 μm ($\overline{X}$ = 18.3 μm, n = 10) and a minor axis between 6.0 μm to 16.4 μm ($\overline{X}$ = 12.8 μm, n = 10) and could only be discerned by its marginally fainter colour compared to the rest of the cell. The cell surface had longitudinal arrays of epicytic folds at a density of 3 folds/μm (Fig. 2C). The mucron was triangular and formed an angled protrusion at the anterior (Fig. 2D). Gliding motility was observed. Isolated from *Asterocarpa humilis* Heller, 1878.

3.3. Lankesteria savignyii sp. nov.

Cells narrowly obpanduriform with tapering posterior and anterior ends that flanked a fat center that bulged markedly in some individuals (Fig. 3A, B). The general coloration was gray to light brown with a translucent mucron. Trophozoite sizes ranged between 48.5 and 85.8 μm ($\overline{X}$ = 68.7 μm, n = 40) in length and 14.9 to 35.0 μm ($\overline{X}$ = 23.5 μm, n = 40) in width at the widest point of the cell. The nucleus was oval and situated within the first third of the anterior of the cell with a major axis between 8.0 and 12.1 μm ($\overline{X}$ = 9.4 μm, n = 20) and a minor axis between 6.1 and 10.4 μm ($\overline{X}$ = 8.2 μm, n = 20). The cell surface comprised of epicytic folds arranged longitudinally at a density of 3 folds/μm (Fig. 3C). Furthermore, these folds were spaced apart and appeared superficial compared to the typical density and depth of epicytic folds observed in other species. The mucron formed a protrusion that was capped by a small bump (Fig. 3B, D). Gliding motility was observed. Isolated from *Ciona savignyi* Herdman, 1882.

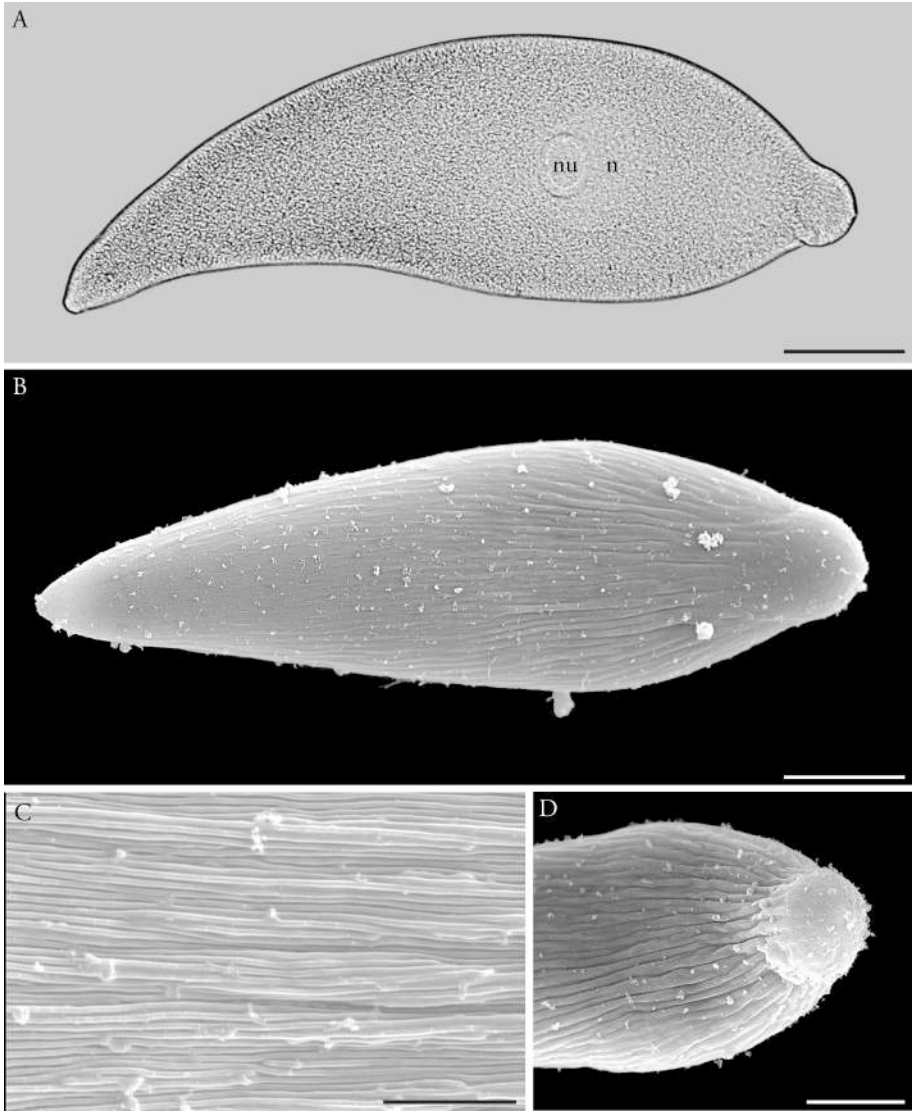

Fig. 1. Light micrograph (LM) and scanning electron micrographs (SEM) of *Lankesteria kaiteriteriensis* sp. nov. showing trophozoite morphology. Mucron oriented to the right. (A) LM of trophozoite taken in differential interference contrast (DIC). Very narrowly to narrowly spatulate cell bent in a crescent shape with an oval nucleus (n) situated in the anterior third of the body with a distinct nucleolus (nu). The mucron is transparent and stubby. (B) SEM of the trophozoite showing overall shape and morphology. (C) SEM of epicytic folds forming a longitudinal array at a density of 4 folds/μm (D) SEM of the anterior portion of the cell including the mucron. Scale bars: A, B = 30 μm; C = 3 μm; D = 15 μm.

3.4. *Lankesteria pollywoga sp. nov.*

Trophozoites narrowly obpyriform with a tapering, rod-like body beginning with a spherical anterior like a tadpole or roughly the overall shape of a medieval mace (Fig. 4A, B). Posterior end and mucron translucent, but the remainder of the cell golden-brown. The cells ranged between 96.6 and 155.1 μm ($\overline{X}$ = 118.4 μm, n = 40) in length and 25.2 to 43.6 μm ($\overline{X}$ = 34.7 μm, n = 40) in width at the widest point of the cell. A nearly circular nucleus that measured between 13.2 and 21.1 μm ($\overline{X}$ = 18.4 μm, n = 20) by 12.7 to 19.4 μm ($\overline{X}$ = 16.1 μm, n = 20) was located approximately one fifth of the total body length from the anterior of the cell. The nucleolus, placed at the anterior end of the nucleus, was also circular and measured between 4.2 and 11.9 μm ($\overline{X}$ = 7.3 μm, n = 20) in diameter. The cell surface comprised of epicytic folds arranged longitudinally at a density of 3–4 folds/μm (Fig. 4C). The mucron consisted of a protrusion that bent ventrally which could be clearly seen from a lateral view (Fig. 4D). Gliding motility was observed. Isolated from *Molgula complanata* Alder & Hancock, 1870.

3.5. *SSU rDNA sequences and phylogenetic analyses*

The 90-taxon alignment of SSU rDNA sequences yielded the dinoflagellates (98% Maximum likelihood bootstrap [MLB], 1.00 Bayesian posterior probability [BPP]) and an ingroup of apicomplexans sorted into broad groups situated on a poorly resolved backbone (Fig. 5). Both maximum likelihood and Bayesian analyses recovered identical tree topologies. The deepest apicomplexan nodes included the piroplasmid, coccidian, rhytidocystid, cryptosporidian, and gregarine clades. The terrestrial gregarines were recovered in two separate clades: terrestrial gregarines I (94 MLB, 1.00 BPP) and terrestrial gregarines II (100 MLB, 1.00 BPP). The marine eugregarines (69 MLB, 0.99 BPP) formed a sister clade to terrestrial gregarine Clade II and included the capitellid gregarines, urosporids, lecudininds, *Difficilina*, *Veloxidium*, paralecudinids. Archigregarines were unresolved with *Selenidium* forming three separate branches. The sipunculid gregarines formed a separate, early branching clade.

The SSU rDNA sequences that were obtained for each of the novel species included in this study formed distinct branches within the lecudinids (Fig. 5). *Lankesteria pollywoga* sp. nov. clustered in an early branching clade (100 MLB, 1.00 BPP) relative to *Le. longissima*, *Le. phyllochaetopterii*, *Le. tuzetae*, and *La. abbotti*. *Lankesteria savignyii* sp. nov. formed a sister lineage to *La. ascidiae* (100 MLB, 1.00 BPP), the type species for *Lankesteria*, and these two species formed a clade with *La. cystodytae* (90 MLB, 1.00 BPP). *Lankesteria dolabra* sp. nov. and *La. kaiteriteriensis* sp. nov. were recovered as sister taxa to each other (94 MLB, 1.00 BPP), but the phylogenetic position of these two species in the

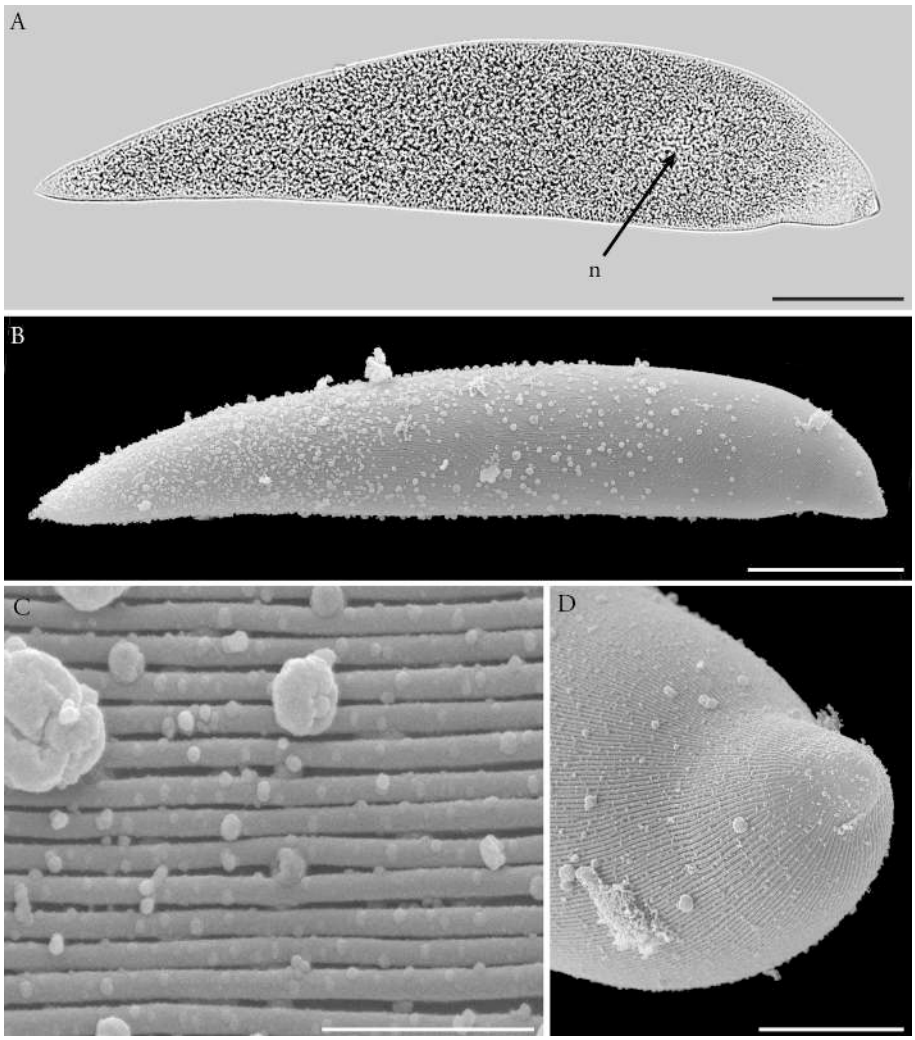

Fig. 2. Light micrograph (LM) and scanning electron micrographs (SEM) of *Lankesteria dolabra* sp. nov. showing trophozoite morphology. Mucron oriented to the right. (A) LM of trophozoite taken in differential interference contrast (DIC). Very narrowly spatulate cell with inconspicuous nucleus (n) situated in the anterior fifth of the body. (B) SEM of the trophozoite showing overall shape and morphology. (C) SEM of epicytic folds forming a longitudinal array at a density of 3 folds/μm (D) SEM of the anterior portion of the cell including the mucron which protrudes at an angle from the body. Scale bars: A, B = 30 μm; C = 2 μm; D = 10 μm.

context of the lecudinid topology is uncertain.

Lankesteria spp. and *Lecudina* spp. did not form two separate clades. Instead, the overall topology of the lecudinids consisted of a highly supported clade comprised of *Lankesteria* spp. and *Lecudina* spp. mixed together (100 MLB, 1.00 BPP; Fig. 5, Key node 1). The type species for *Lecudina*, *Le. pellucida*, was sister to *Le. caspera* (91 MLB, 1.00 BPP) and was nested within a strongly supported clade of *Lankesteria* spp. (99 MLB, 1.00 BPP; Fig. 5, Key node 2). Similarly, *La. ascidiae* (*Lankesteria* type species) did not form a clade that includes all other *Lankesteria* species. Instead, *La. abbotti,* and *La. pollywoga* sp. nov. diverged early in the topology in unresolved positions along with *Le. tuzetae*, *Le. longissima,* and *Le. phyllochaetopteri.*

4. Discussion

4.1. Systematic and taxonomic considerations for La. Kaiteriteriensis sp. nov., La. Dolabra sp. nov., La. Savignyii sp. nov., La. Pollywoga sp. nov.

Lankesteria kaiteriteriensis sp. *nov.* and *La. dolabra* sp. *nov.* were recovered as sister species based on the molecular phylogenetic data. The two species are morphologically dissimilar with *La. kaiteriteriensis* sp. *nov.* trophozoites possessing a narrowly spatulate shape that arches to an overall crescent shape whereas *La. dolabra* sp. *nov.* trophozoites are very narrowly spatulate and taper to a sharp point at both the posterior and anterior ends. Their size ranges also do not overlap; *La. kaiteriteriensis* sp. *nov.* was 268 μm long and 27 μm wide on average compared to *La. dolabra* sp. *nov.* which measured 174 μm long and 33 μm wide. Furthermore, each species was isolated from different hosts from separate localities.

La. kaiteriteriensis sp. nov. shares general similarities in morphology with *La. montereyensis* and *La. synoici* in terms of overall cell shape. Unfortunately, there is no molecular identity currently available for either of these two species. *Lankesteria montereyensis* is described as being lanceolate to ovoid ranging between 55 μm long and 25 μm in size (Levine, 1981). *Lankesteria synoici*, on the other hand, is described as broadly lanceolate, ovoid, or piriform with a bulbous anterior and a tapering posterior. The overall size of a mature *La. synoici* trophozoite is reported as 81 μm long and 35 μm wide (Levine, 1981). *Lankesteria kaiteriteriensis* sp. nov. is longer than either species measuring 268 μm long on average. Moreover, *La. kaiteriteriensis* sp. nov. arches to a crescent shape whereas the descriptions and line drawings for *La. monetereyensis* and *La. synoici* do not depict such curvature. Finally, *La. kaiteriteriensis* sp. nov. was isolated from *Pyura* sp. in New Zealand whereas both *La. monetereyensis* and *La. synoici* were isolated from colonial ascidians in California; *Archidistoma molle* and *Synoicum parfustis* respectively. Due to these differences, *La. kaiteriteriensis* sp. nov., is distinct from *La. monetereyensis* and *La. synoici*.

Lankesteria dolabra sp. nov. is superficially similar to *La. halocynthiae* in general appearance. Both species taper to a point at both the anterior and posterior ends with the description for *La. halocynthiae* including a flattened peapod shape measuring 227 μm long and 53 μm wide (Rueckert et al., 2015). Beyond the similarity in shape, however, there

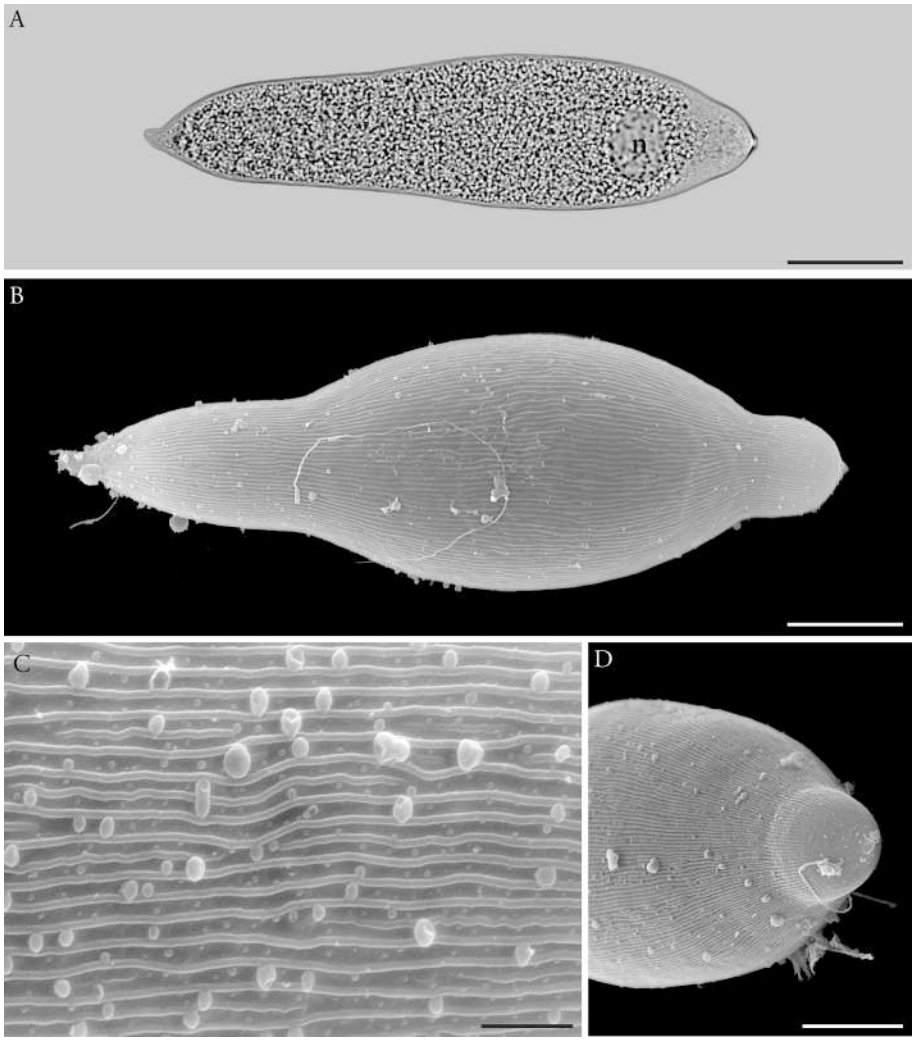

Fig. 3. Light micrograph (LM) and scanning electron micrographs (SEM) of *Lankesteria savignyii* sp. nov. showing trophozoite morphology. Mucron oriented to the right. (A) LM of trophozoite taken in differential interference contrast (DIC). Narrowly obpanduriform cell with oval nucleus (n) situated in the anterior sixth of the body. (B) SEM of the trophozoite showing overall shape and morphology. (C) SEM of epicytic folds forming a longitudinal array at a density of 3 folds/μm (D) SEM of the anterior portion of the cell including the small mucron. Scale bars: A, B = 10 μm; C = 2 μm; D = 10 μm.

are many distinguishing differences between *La. dolabra* sp. nov. and *La. halocynthiae*. *Lankesteria dolabra* sp. nov. is smaller in average size measuring 174 μm long and 33 μm wide and does not possess a distinct halfmoon-shaped nucleus as in is the case for *La. halocynthiae*. Furthermore, *La. dolabra* sp. nov. and *La. halocynthiae* are found in different hosts from different localities, *Asterocarpa humilis* from New Zealand and *Halocynthia aurantium* from Canada respectively, and are genetically distinct in the molecular phylogeny.

Considering the differences between *La. kaiteriteriensis* sp. nov. and *La. dolabra* sp. nov to each other and to other superficially similar species, both species are taxonomically distinct. Molecular phylogenetics also showed that the two new species cluster with their respective single isolate sequences in the molecular phylogenies. Therefore, both *La. kaiteriteriensis* sp. *nov.* and *La. dolabra* sp. *nov.* represent novel species within *Lankesteria*.

Lankesteria savignyii sp. nov. and *La. ascidiae* were robustly supported as sister species in both the 90 and 48-taxon phylogenies. Interestingly, *Ciona savignyi* and *C. intestinalis*, the hosts for both gregarine taxa, are also sister species (Stach and Turbeville, 2002; Turon and López-Legentil, 2004). A significant morphological difference between *La. savignyii* sp. *nov.* and *La. ascidiae* is the general trophozoite shape: *La. savignyii* sp. *nov.* is narrowly obpanduriform with a fat, bulging center that tapers to a narrow anterior whereas *La. ascidiae* is either described, hand-drawn, or photographed as a clavate cell with a round anterior (Ciancio et al., 2001; Levine, 1981; Mita et al., 2012). Additionally, the surface of *La. ascidiae* is described as having rows of knobs with few epicytic folds appearing mostly in the posterior of the trophozoite (Mita et al., 2012); both of these characteristics are not consistent with the morphology observed for *La. savignyii* sp. nov. The sizes of the two species overlap: *La. savignyii* sp. *nov.* measured 69 μm long and 23 μm wide on average compared to *La. ascidiae* which measures 50–99 pm long, 20–30 pm wide (Levine, 1981) or 62 μm long, 19 μm wide (Mita et al., 2012). Furthermore, both species were found in the intestine of their respective hosts and were capable of gliding motility.

The molecular phylogenetic analysis, however, shows that the separate *La. savignyii* sp. nov. isolates cluster with each other and exclude the *La. ascidiae* sequence. There was also a 2.6% (p-distance) divergence in SSU rDNA between *La. savignyii* sp. *nov.* and *La. ascidiae*. A previous study on new *Lankesteria* species observed similar interspecific divergence (2.1–3.1%; Rueckert and Leander, 2008). Additionally, *La. savignyii* sp. *nov.* infects *C. savignyi* and has not been observed in previous investigations of *C. intestinalis* by other authors. Therefore, these data suggest that *La. savignyii* sp. *nov.* is distinct from *La. ascidiae*.

Lankesteria pollywoga sp. nov. was recovered in an early diverging position within the lecudinids. Morphologically, *La. pollywoga* sp. nov. shares general similarities with the line drawings of *La. diaphanis* and *La. pittendrighi* (Levine, 1981); these species do not currently have molecular identities and were thus not included in the molecular phylogenetic analysis. The trophozoite stage of *Lankesteria diaphanis* is described as being brownish overall with an elongated body ending in a mucron which often bears a small knob at the anterior end. Although *La. pollywoga* sp. nov. shares the overall shape and brownish colouration, *La.*

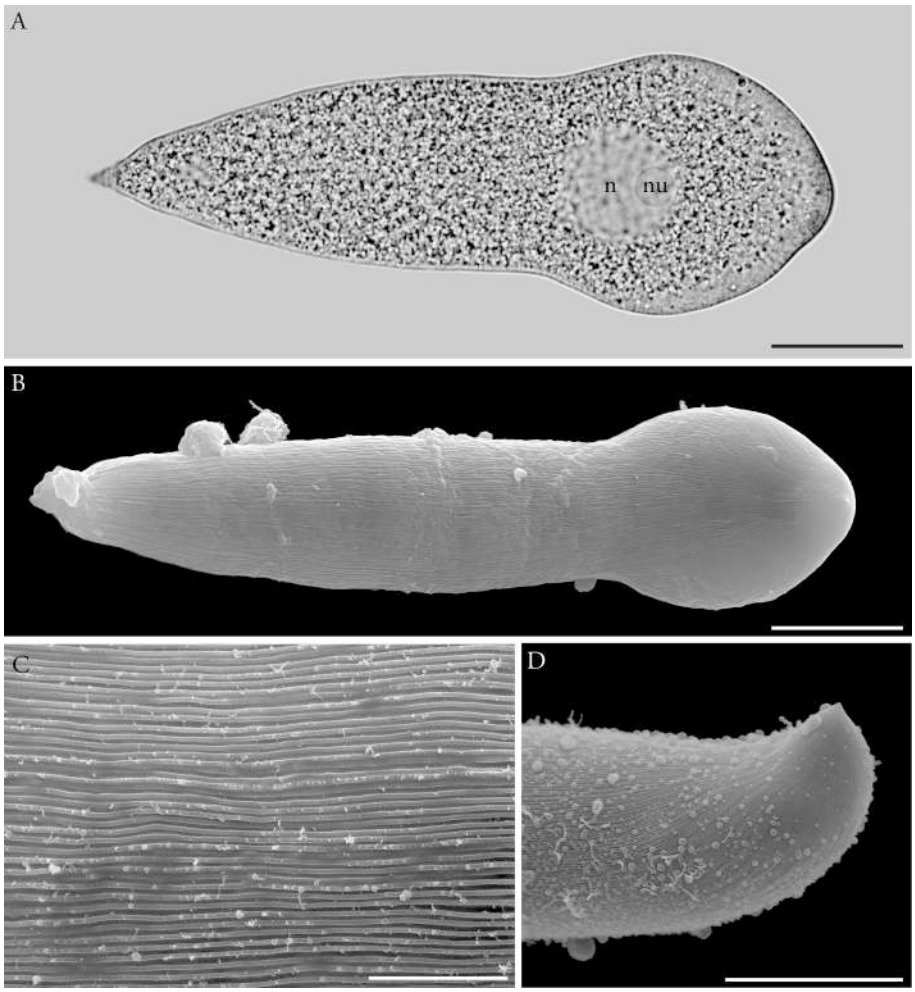

Fig. 4. Light micrograph (LM) and scanning electron micrographs (SEM) of *Lankesteria pollywoga* sp. nov. showing trophozoite morphology. Mucron oriented to the right. (A) LM of trophozoite taken in differential interference contrast (DIC). Narrowly obpyriform, tadpole-shaped cell with nucleus (n) and nucleolus (nu) situated in the anterior fifth of the body. (B) SEM of the trophozoite showing overall shape and morphology. (C) SEM of epicytic folds forming a longitudinal array at a density of 3–4 folds/μm (D) SEM of the anterior portion of the cell including an inconspicuous mucron that bends ventrally and is most observable from a lateral view. Scale bars: A, B = 20 μm; C = 5 μm; D = 20 μm.

diaphanis is smaller measuring 78 μm long by 17–30 μm wide compared to *La. pollywoga* sp. *nov.* which measures 118 μm long by 35 μm on average. Moreover, *La. diaphanis* is capable of metabolic movement, which was not observed in *La. pollywoga* sp. *nov.* The hosts are also different as *La. diaphanis* was isolated from the colonial ascidian *Eudistoma diaphanes* in California. *Lankesteria pittendrighi* trophozoites are described as being brownish with a broadly lanceolate body or with an anterior swelling starting near the anteriorly positioned nucleus (Levine, 1981). *Lankesteria pittendrighi* is, however, smaller than *La. pollywoga* sp. *nov.*, measuring 52–60 μm long by 23–31 μm. Additionally, the host is different as *Lankesteria pittendrighi* was isolated from the solitary sea squirt *Ascidia ceratodes* in California.

Lankesteria pollywoga sp. nov., therefore, is distinguishable from previously described species in terms of size, host species, and the lack of metabolic movement. Furthermore, although the position of the *La. pollywoga* sp. *nov.* lineage is uncertain on the molecular phylogeny, there is high support for *La. pollywoga* sp. *nov.* sequences clustering amongst each other to the exclusion of other known sequences. These data, therefore, strongly suggest that *La. pollywoga* sp. *nov.* is a new species of *Lankesteria.*

4.2. Systematics and evolutionary history of Lankesteria and Lecudina

Early molecular phylogenetic studies supported the distinction between *Lankesteria* and *Lecudina.* In contrast, the molecular phylogenetic analysis from the present study does not recover these genera as clades and reveals a taxonomic problem whereby *Lecudina* species are scattered and distributed within *Lankesteria* clades. Both genera are unified (Fig. 5, Key node 1) with *Lecudina* species scattered amongst *Lankesteria* as follows: *Le. longissima* and *Le. phyllochaetopteri* as sister taxa in an early diverging position within the lecudinids; *Le. pellucida*, the type species of *Lecudina*, as sister to *Le. caspera* and nested within a highly supported clade of *Lankesteria* species; *Le. tuzetae* as sister to *La. abbotti*. The placement of *Le. pellucida* within a strongly supported clade of *Lankesteria* species (Fig. 5, Key node 2) offers evidential support for the problematic classification of *Lecudina* and *Lankesteria* as separate genera. Previously published marine eugregarine phylogenies (e.g., Iritani et al., 2017; Rueckert et al., 2015; Rueckert and Leander, 2008; Schrével et al., 2016) likely did not detect the problematic distribution of *Lecudina* species simply because these studies employed datasets that were comprehensive for a specific clade of concern, but molecular datasets for *Lankesteria* and *Lecudina* were quite limited.

The nested placement of *Le. pellucida* within a clade of *Lankesteria*, as seen in the present study, suggests that *Lankesteria* and *Lecudina* represent genera that do not reflect phylogeny. Many of the morphological criteria used for taxonomy to diagnose *Lankesteria* and *Lecudina* are qualitative and subjective. These characters for *Lankesteria* include a mucron of variable complexity, present although not always apparent; more or less spatulate trophozoites; head-to-head or scissors-like syzygy; spherical gametocysts; anisogamy present; ellipsoidal oocysts, often with a plug at each end; and parasitism of ascidians (Levine, 1977). Other authors have also included a brownish coloration associated with the accumulation of amylopectin granules in the cytoplasm, the infection occurring within the host intestine or stomach, and gliding motility (Desportes and Schrével, 2013; Levine, 1981; Mita et al., 2012; Rueckert et al., 2015; Rueckert and Leander, 2008) as important characters. In

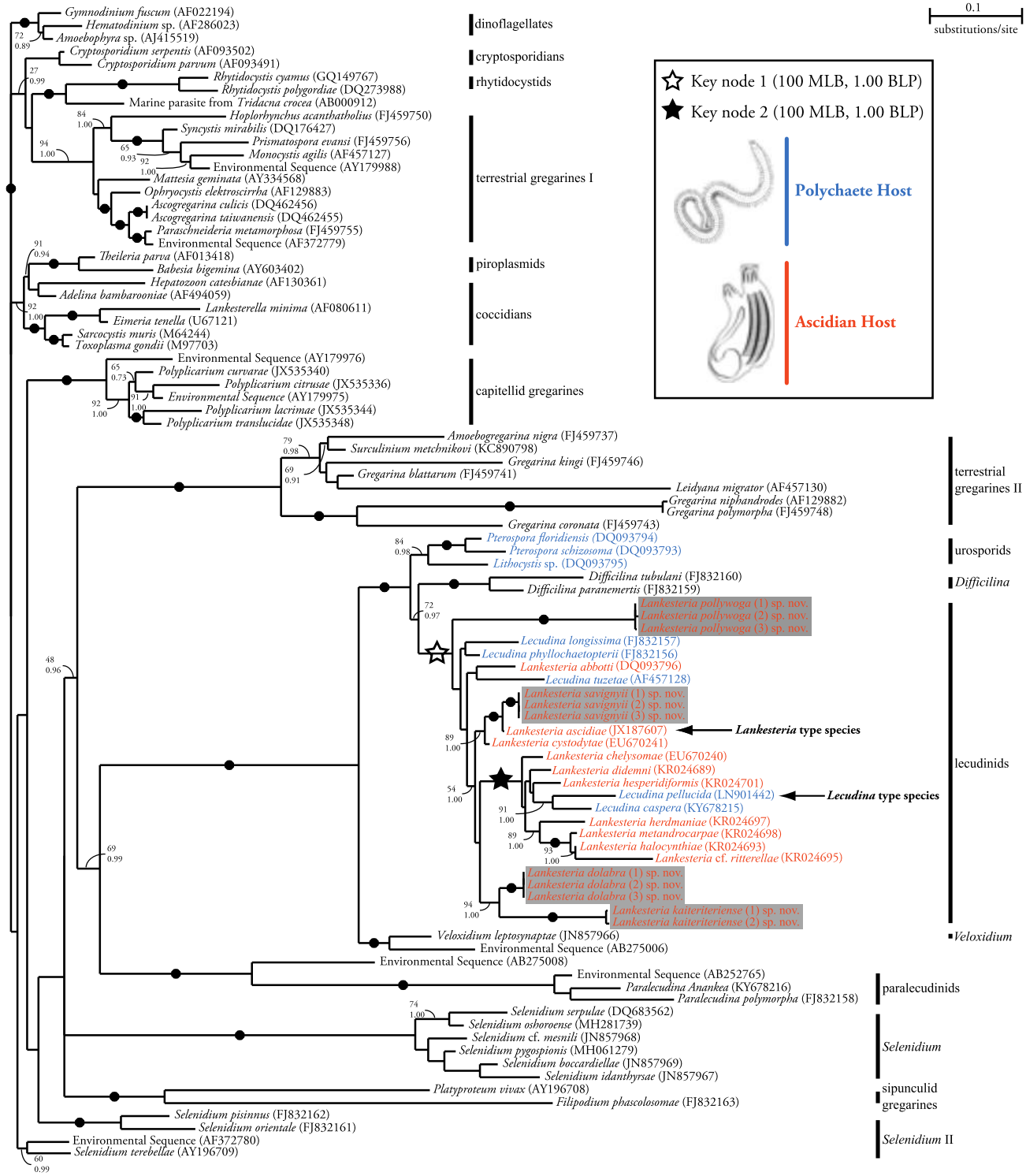

Fig. 5. Maximum likelihood phylogeny inferred from a 90 taxa dataset of SSU rDNA sequences with 1,440 unambiguously aligned sites using the GTR + I + Γ model of substitution (proportion of invariable sites = 0.1970, gamma shape = 0.6960). Numbers indicate bootstrap support (top value) and Bayesian posterior probability (bottom value). Black dots on branches denote when both bootstrap support and Bayesian posterior probabilities were equal to or > 95 and 0.99 respectively. Branches without support values had bootstrap support and Bayesian posterior probabilities below 60 and 0.95 respectively. White star (key node 1) marks the *Lankesteria* spp. and *Lecudina* spp. clade. The black star (key node 2) marks the clade comprised of the *Lecudina* type species nested within *Lankesteria*. Taxa in blue are parasites of polychaete hosts whereas taxa in orange are parasites of ascidian hosts. The new species described in the current study are highlighted with gray boxes. (For interpretation of the references to colour in this figure legend, the reader is referred to the web version of this article.)

contrast, the diagnostic criteria for *Lecudina* include a simple mucron without hooks or exfoliations, trophozoites without myonemes, ovoid oocysts which are thickened at one end, and parasitism of polychaetes and other marine invertebrates (Levine, 1976). The mixed distribution of *Lankesteria* and *Lecudina* species recovered in the present study suggests that these morphological characters can perhaps be applied to lecudinid parasites of ascidians or polychaetes respectively, but are not phylogenetically informative.

From an evolutionary standpoint, it can be inferred that the most recent ancestor to the lecudinids was a parasite of polychaetes based on how other gregarines that infect polychaetes (e.g., paralecudinids, *Pterospora*, *Selenidium*) occupy deeper nodes. The switch to ascidian parasitism was made at the base of the *Lecudina* clade (Fig. 5, Key node 1) although the precise topology remains unresolved. Morphological resemblance between *Lecudina* parasites of polychaete hosts deep in the phylogeny to those species nested within ascidian parasites is perhaps due to convergence following a secondary switch to polychaete hosts.

The confounded distinction between *Lankesteria* and *Lecudina* should be addressed for taxonomic clarity and for a better reflection of phylogeny. The construction of multi-gene phylogenies (e.g., SSU and LSU rDNA) that include additional novel taxa and type species, in conjunction with a parasitological approach to further investigate host specificity, are critical to obtaining a deeper understanding of whether these two genera are taxonomically sound.

4.3. Taxonomic summary

Phylum Apicomplexa Levine, 1970
Order Eugregarinorida Léger, 1900
Family Lecudinidae Kamm, 1922
Lankesteria Mingazzini 1891

4.3.1. *Lankesteria kaiteriteriensis sp. nov.*

Description Very narrowly to narrowly spatulate trophozoites bend to an overall crescent shape and ranged between 165.3 and 405.7 μm ($\overline{X}$ = 268.0 μm, n = 80) in length and 32.7 to 114.6 μm ($\overline{X}$ = 50.0 μm, n = 80) in width. Dark brown posterior gradually turns light gray near the nucleus. Silver to translucent mucron is conspicuous and stubby. Oval nucleus with a major axis 38.5 to 71.7 μm ($\overline{X}$ = 56.3 μm, n = 20) and a minor axis between 35.7 and 66.0 μm ($\overline{X}$ = 49.6 μm, n = 20) situated in the first anterior third of the cell body. Distinct nucleolus forms a ring measuring 14.8 to 31.6 μm ($\overline{X}$ = 25.4 μm, n = 20) by 17.2 to 29.7 μm ($\overline{X}$ = 23.7 μm, n = 80). Longitudinal epicytic folds line the cell surface at 4 folds/μm. Gliding motility.

DNA sequence. SSU rDNA sequence (GenBank MW748138).
Type locality. Kaiteriteri Beach, Kaiteriteri, New Zealand (41°02′07.7″S 173°01′21.4″E). Host commonly found on the underside or cracks of large (~1 m diameter) rocks in the low intertidal to subtidal zones.
Type habitat. Marine
Type host. *Pyura* sp. Molina, 1782 (Chordata, Tunicata, Ascidiacea, Stolidobranchia, Pyuridae)
Location in host. Intestinal lumen
Iconotype. Fig. 1A
Hapantotype. Trophozoites on SEM stubs with a gold/palladium alloy sputter coat have been stored in the algal and protist collection in the Hokkaido University Museum (DI – 2).
LSID. A8AC1E44-8D15-40CB-929E-E4DE582BAC1C
Etymology. Species name refers to the type locality of Kaiteriteri, New Zealand.

4.3.2. *Lankesteria dolabra sp. nov.*

Description. Very narrowly spatulate trophozoites consisting of rod-like body and tapering posterior ending in a sharp point. Both posterior end and mucron are transparent; cell body is light golden brown. Trophozoites range between 163.7 and 207.1 μm ($\overline{X}$ = 173.7 μm, n = 40) in length and 22.7 to 43.5 μm ($\overline{X}$ = 32.6 μm, n = 40) in width. Faint, inconspicuous nucleus with a major axis between 14.4 and 21.9 μm ($\overline{X}$ = 18.3 μm, n = 10) and a minor axis between 6.0 μm to 16.4 μm ($\overline{X}$ = 12.8 μm, n = 10) situated in the first anterior fifth of trophozoite body. Mucron is translucent, bent, and ends in point. Cell surface constituted by longitudinal epicytic folds at a 3 folds/μm density. Gliding motility.

DNA sequence. SSU rDNA sequence (GenBank MW748137).
Type locality. Waikawa Marina, Marlborough, New Zealand (41°16′02.8″S 174°02′18.4″E). Host commonly found on fouled ropes submerged off the side of docks.

Type habitat. Marine
Type host. *Asterocarpa humilis* Heller, 1878 (Chordata, Tunicata, Ascidiacea, Stolidobranchia, Styelidae)
Location in host. Intestinal lumen
Iconotype. Fig. 2A
Hapantotype. Trophozoites on SEM stubs with a gold/palladium alloy sputter coat have been stored in the algal and protist collection in the Hokkaido University Museum (DI – 3).
LSID. A989F5C9-4F99-4DAD-A07A-82CF4EDD1F0F
Etymology. Species name refers to the morphological resemblance of the trophozoite to the head of a pickaxe or dolabra.

4.3.3. *Lankesteria savignyii sp. nov.*

Description. Trophozoites narrowly obpanduriform with a tapering posterior and anterior. Body is fat and bulges markedly in some individuals. Gray to light brown with a translucent mucron. Trophozoites range between 48.5 and 85.8 μm ($\overline{X}$ = 68.7 μm, n = 40) in length and 14.9 to 35.0 μm ($\overline{X}$ = 23.5 μm, n = 40) in width. Oval nucleus situated within the first sixth of the cell from the anterior with a major axis between 8.0 and 12.1 μm ($\overline{X}$ = 9.4 μm, n = 20) and a minor axis between 6.1 and 10.4 μm ($\overline{X}$ = 8.2 μm, n = 20). Translucent mucron capped with small bump. Cell surface comprised of superficial longitudinal epicytic folds at a 3 folds/μm density. Gliding motility.

DNA sequence. SSU rDNA sequence (GenBank MW748136).
Type locality. Nelson Marina, Nelson, New Zealand (41°15′37.1″S 173°16′53.0″E) on fouled ropes hanging from the docks.
Type habitat. Marine
Type host. *Ciona savignyi* Herdman, 1882 (Chordata, Tunicata, Ascidiacea, Phlebobranchia, Cionidae).
Location in host. Intestinal lumen
Iconotype. Fig. 3A
Hapantotype. Trophozoites on SEM stubs with a gold/palladium alloy sputter coat have been stored in the algal and protist collection in the Hokkaido University Museum (DI – 4).
LSID. 9A838F5F-0BA3-47C7-8D2E-E2ACEADF71D2
Etymology. Species name refers to the name of the host: *Ciona savignyi* Herdman, 1822

4.3.4. *Lankesteria pollywoga sp. nov.*

Description. Narrowly obpyriform trophozoites with elongated, rod-like body ending in a spherical anterior. Golden-brown overall with translucent posterior and mucron. Trophozoites between 96.6 and 155.1 μm ($\overline{X}$ = 118.4 μm, n = 40) in length and 25.2 to 43.6 μm ($\overline{X}$ = 34.7 μm, n = 40) in width. Circular nucleus between 13.2 and 21.1 μm ($\overline{X}$ = 18.4 μm, n = 20) by 12.7 to 19.4 μm ($\overline{X}$ = 16.1 μm, n = 20) located one fifth of the total body length from anterior. Circular nucleolus measures between 4.2 and 11.9 μm ($\overline{X}$ = 7.3 μm, n = 20) in diameter and is situated at the anterior portion of nucleus. Translucent mucron bends ventrally and is seen clearly from a lateral view. Cell surface comprised of longitudinal epicytic folds at a 3–4 folds/μm density. Gliding motility.

DNA sequence. SSU rDNA sequence (GenBank MW748135).
Type locality. Nelson Marina, Nelson, New Zealand (41°15′37.1″S 173°16′53.0″E) on fouled ropes hanging from the docks.
Type habitat. Marine
Type host. *Molgula complanata* Alder & Hancock, 1870
Location in host. Intestinal lumen
Iconotype. Fig. 4A

Hapantotype. Trophozoites on SEM stubs with a gold/palladium alloy sputter coat have been stored in the algal and protist collection in the Hokkaido University Museum (DI – 5).
LSID. 578FEC9B-0963-45D8-8D7F-162A6A29FAD7
Etymology. Species name refers to the morphological resemblance of the trophozoite to both a tadpole and a stage two Demogorgon (i.e., pollywog in both cases) from the hit Netflix series Stranger Things (Season 2, Episode 3).

Declaration of Competing Interest

The authors declare that they have no known competing financial interests or personal relationships that could have appeared to influence the work reported in this paper.

Acknowledgements

This research was supported by a MEXT doctoral scholarship to Davis Iritani, and a joint JSPS/MBIE-RSZN (PG6R180004) provided to Kevin Wakeman, Steve Webb, and Jonathan Banks. We are grateful to the Electron Microscope Laboratory, Research Faculty of Agriculture, Hokkaido University for sharing their critical point dryer, and to Dr. Katrina-Kay Alaimo for providing her expertise in classical Latin and Greek.

References

Abrahamsen, M.S., Templeton, T.J., Enomoto, S., Abrahante, J.E., Zhu, G., Lancto, C.A., Deng, M., Liu, C., Widmer, G., Tzipori, S., Buck, G.A., Xu, P., Bankier, A.T., Dear, P. H., Konfortov, B.A., Spriggs, H.F., Iyer, L., Anantharaman, V., Aravind, L., Kapur, V., 2004. Complete Genome Sequence of the Apicomplexan , Cryptosporidium parvum. Science. 304, 441–445. https://doi.org/10.1126/science.1094786.

Adl, S.M., Bass, D., Lane, C.E., Lukeš, J., Schoch, C.L., Smirnov, A., Agatha, S., Berney, C., Brown, M.W., Burki, F., Cárdenas, P., Čepička, I., Chistyakova, L., del Campo, J., Dunthorn, M., Edvardsen, B., Eglit, Y., Guillou, L., Hampl, V., Heiss, A.A., Hoppenrath, M., James, T.Y., Karnkowska, A., Karpov, S., Kim, E., Kolisko, M., Kudryavtsev, A., Lahr, D.J.G., Lara, E., Le Gall, L., Lynn, D.H., Mann, D.G., Massana, R., Mitchell, E.A.D., Morrow, C., Park, J.S., Pawlowski, J.W., Powell, M.J., Richter, D.J., Rueckert, S., Shadwick, L., Shimano, S., Spiegel, F.W., Torruella, G., Youssef, N., Zlatogursky, V., Zhang, Q., 2019. Revisions to the Classification, Nomenclature, and Diversity of Eukaryotes. J. Eukaryot. Microbiol. 66, 4–119. https://doi.org/10.1111/jeu.12691.

Adl, S.M., Leander, B.S., Simpson, A.G.B., Archibald, J.M., Anderson, O.R., Bass, D., Bowser, S.S., Brugerolle, G., Farmer, M. a, Karpov, S., Kolisko, M., Lane, C.E., Lodge, D.J., Mann, D.G., Meisterfeld, R., Mendoza, L., Moestrup, Ø., Mozley-Standridge, S. E., Smirnov, A. V, Spiegel, F., 2007. Diversity, nomenclature, and taxonomy of protists. Syst. Biol. 56, 684–689. https://doi.org/10.1080/10635150701494127.

Adl, S.M., Simpson, A.G.B., Lane, C.E., Lukeš, J., Bass, D., Bowser, S.S., Brown, M.W., Burki, F., Dunthorn, M., Hampl, V., Heiss, A., Hoppenrath, M., Lara, E., Gall, L. Le, Lynn, D.H., McManus, H., Mitchell, E.A.D., Mozley-Stanridge, S.E., Parfrey, L.W., Pawlowski, J., Rueckert, S., Shadwick, L., Schoch, C.L., Smirnov, A., Spiegel, F.W., 2012. The revised classification of eukaryotes. J. Eukaryot. Microbiol. 59, 429–493. https://doi.org/10.1111/j.1550-7408.2012.00644.

Ciancio, A., Scippa, S., Cammarano, M., 2001. Ultrastructure of trophozoites of the gregarine Lankesteria ascidiae (Apicornplexa: Eugregarinida) parasitic in the ascidian *Ciona intestinalis* (protochordata). Eur. J. Protistol. 37, 327–336. https://doi.org/10.1078/0932-4739-00829.

Clopton, R.E., 2004. Standard Nomenclature and Metrics of Plane Shapes for Use in Gregarine Taxonomy. Comp. Parasitol. 71, 130–140. https://doi.org/10.1654/4151.

Darriba, D., Taboada, Guillermo L, Doallo, R., Posada, D., 2012. jModelTest 2: more models, new heuristics and parallel computing. Nat. Methods 9, 772. https://doi.org/10.1038/nmeth.2109.

Desportes, I., Schrével, J., 2013. The Gregarines, in: Treatise on Zoology-Anatomy, Taxonomy, Biology. Koninklijke Brill NV, Leiden.

Folmer, O., Black, M., Hoeh, W., Lutz, R., Vrijenhoek, R., 1994. DNA primers for amplification of mitochondrial cytochrome c oxidase subunit I from diverse metazoan invertebrates. Mol. Mar. Biol. Biotechnol. 3, 294–299.

Grassé, P.P., 1953. Classe des Grégarinomorphes (Gregarinomorpha, N. nov., Grégarinae Haeckel, 1866; Grégarinidea Lankester, 1885; Grégarines des auteurs). In Traité de Zoologie. Paris.

Guindon, S., Gascuel, O., 2003. A simple, fast, and accurate algorithm to estimate large phylogenies by maximum likelihood. Syst. Biol. 52, 696–704. https://doi.org/10.1080/10635150390235520.

Iritani, D., Wakeman, K., Leander, B.S., 2017. Molecular Phylogenetic Positions of Two New Marine Gregarines (Apicomplexa) - *Paralecudina anankea* n. sp. and *Lecudina caspera* n. sp. - from the Intestine of *Lumbrineris inflata* (Polychaeta) Show Patterns of Co-evolution. J. Eukaryot. Microbiol. 1–9 https://doi.org/10.1111/jeu.12462.

Katoh, K., Misawa, K., Kuma, K., Miyata, T., 2002. MAFFT: a novel method for rapid multiple sequence alignment based on fast Fourier transform. Nucleic Acids Res. 30, 3059–3066. https://doi.org/10.1093/nar/gkf436.

Kim, K., Weiss, L.M., 2004. *Toxoplasma gondii*: The model apicomplexan. Int. J. Parasitol. 34, 423–432. https://doi.org/10.1016/j.ijpara.2003.12.009.

Kück, P., Meusemann, K., Dambach, J., Thormann, B., von Reumont, B.M., Wägele, J.W., Misof, B., 2010. Parametric and non-parametric masking of randomness in sequence alignments can be improved and leads to better resolved trees. Front. Zool. 7, 10. https://doi.org/10.1186/1742-9994-7-10.

Kumar, S., Stecher, G., Tamura, K., 2016. MEGA7: Molecular Evolutionary Genetics Analysis version 7.0 for bigger datasets. Mol. Biol. Evol. 33, msw054. https://doi.org/10.1093/molbev/msw054.

Lambert, G., 2007. Invasive sea squirts: A growing global problem. J. Exp. Mar. Bio. Ecol. 342, 3–4. https://doi.org/10.1016/j.jembe.2006.10.009.

Leander, B.S., 2008. Marine gregarines: evolutionary prelude to the apicomplexan radiation? Trends Parasitol. 24, 60–67. https://doi.org/10.1016/j.pt.2007.11.005.

Leander, B.S., 2006. Ultrastructure of the archigregarine *Selenidium vivax* (Apicomplexa) – A dynamic parasite of sipunculid worms (host: Phascolosoma agassizii). Mar. Biol. Res. 2, 178–190. https://doi.org/10.1080/17451000600724395.

Leander, B.S., Clopton, R.E., Keeling, P.J., 2003. Phylogeny of grenarines (Apicomplexa) as inferred from a small-subunit rDNA and ß-tubulin. Int. J. Syst. Evol. Microbiol. 53, 345–354. https://doi.org/10.1099/ijs.0.02284-0.

Levine, N.D., 1981. New Species of *Lankesteria* (Apicomplexa, Eugregarinida) from Ascidians on the Central California Coast. J. Protozool. 28, 363–370. https://doi.org/10.1111/j.1550-7408.1981.tb02868.x.

Levine, N.D., 1977. Revision and Checklist of the Species (Other Than *Lecudina*) of the Aseptate Gregarine Family Lecudinidae. J. Protozool. 24, 41–52. https://doi.org/10.1111/j.1550-7408.1977.tb05279.x.

Levine, N.D., 1976. Revision and Checklist of the Species of the Aseptate Gregarine Genus *Lecudina*. Trans. Am. Microsc. Soc. 95, 695–702. https://doi.org/10.1111/j.1550-7408.1977.tb05279.x.

McKindsey, C.W., Landry, T., O'Beirn, F.X., Davis, I.M., 2007. Bivalve Aquaculture and Exotic Species: a Review of Ecological Considerations and Management Issues. J. Shellfish Res. 26, 281–294. https://doi.org/10.2983/0730-8000(2007)26[281:baaesa]2.0.co;2.

Miller, M.A., Pfeiffer, W., Schwartz, T., 2010. Creating the CIPRES Science Gateway for inference of large phylogenetic trees. 2010 Gatew. Comput. Environ. Work. GCE 2010. https://doi.org/10.1109/GCE.2010.5676129.

Mingazzini, P., 1891. Gregarine monocistidee, nuove o poco conosciute, del Golfo di Napoli. *Atti Ace. Lincei. Rend.* Roma 4, 229–235.

Misof, B., Misof, K., 2009. A Monte Carlo Approach Successfully Identifies Randomness in Multiple Sequence Alignments: A More Objective Means of Data Exclusion. Syst. Biol. 58, 21–34. https://doi.org/10.1093/sysbio/syp006.

Mita, K., Kawai, N., Rueckert, S., Sasakura, Y., 2012. Large-scale infection of the ascidian *Ciona intestinalis* by the gregarine *Lankesteria ascidiae* in an inland culture system. Dis. Aquat. Organ. 101, 185–195. https://doi.org/10.3354/dao02534.

Mo, C., Douek, J., Rinkevich, B., 2002. Development of a PCR strategy for thraustochytrid identification based on 18S rDNA sequence. Mar. Biol. 140, 883–889. https://doi.org/10.1007/s00227-002-0778-9.

Ormières, R., 1965. Recherches sur les sporozoaires parasites des tuniciers. Vie Milieu 15, 823–946.

Page, M., Kelly, M., Herr, B. 2019. Awesome ascidians, a guide to the sea squirts of New Zealand. Niwa, Taihoro Nukurangi. Version 3. https://niwa.co.nz/coasts-and-oceans/marine-identification-guides-and-fact-sheets/seasquirt-id-guide.

Ronquist, F., Teslenko, M., Van Der Mark, P., Ayres, D.L., Darling, A., Höhna, S., Larget, B., Liu, L., Suchard, M.A., Huelsenbeck, J.P., 2012. Mrbayes 3.2: Efficient bayesian phylogenetic inference and model choice across a large model space. Syst. Biol. 61, 539–542. https://doi.org/10.1093/sysbio/sys029.

Rueckert, S., Leander, B.S., 2008. Morphology and phylogenetic position of two novel marine gregarines (Apicomplexa, Eugregarinorida) from the intestines of North-eastern Pacific ascidians. Zool. Scr. 37, 637–645. https://doi.org/10.1111/j.1463-6409.2008.00346.x.

Rueckert, S., Betts, E.L., Tsaousis, A.D., 2019. The Symbiotic Spectrum: Where Do the Gregarines Fit? Trends Parasitol. 35, 687–694. https://doi.org/10.1016/j.pt.2019.06.013.

Rueckert, S., Chantangsi, C., Leander, B.S., 2010. Molecular systematics of marine gregarines (Apicomplexa) from North-eastern Pacific polychaetes and nemerteans, with descriptions of three novel species: *Lecudina phyllochaetopteri* sp. nov., *Difficilina tubulani* sp. nov. and *Difficilina paranemertis* sp. n. Int. J. Syst. Evol. Microbiol. 60, 2681–2690. https://doi.org/10.1099/ijs.0.016436-0.

Rueckert, S., Simdyanov, T.G., Aleoshin, V.V., Leander, B.S., 2011. Identification of a Divergent Environmental DNA Sequence Clade Using the Phylogeny of Gregarine Parasites (Apicomplexa) from Crustacean Hosts. PLoS One 6, e18163. https://doi.org/10.1371/journal.pone.0018163.

Rueckert, S., Wakeman, K.C., Jenke-Kodama, H., Leander, B.S., 2015. Molecular systematics of marine gregarine apicomplexans from Pacific tunicates, with descriptions of five novel species of *Lankesteria*. Int. J. Syst. Evol. Microbiol. 65, 2598–2614. https://doi.org/10.1099/ijs.0.000300.

Rueckert, S., Wakeman, K.C., Leander, B.S., 2013. Discovery of a diverse clade of gregarine apicomplexans (apicomplexa: Eugregarinorida) from pacific eunicid and onuphid polychaetes, including descriptions of *paralecudina* n. gen., *trichotokara japonica* n. sp., and *T. eunicae* n. sp. J. Eukaryot. Microbiol. 60, 121–136. https://doi.org/10.1111/jeu.12015.

Schlüter, D., Däubener, W., Schares, G., Groß, U., Pleyer, U., Lüder, C., 2014. Animals are key to human toxoplasmosis. Int. J. Med. Microbiol. 304, 917–929. https://doi.org/10.1016/j.ijmm.2014.09.002.

Schrével, J., Valigurová, A., Prensier, G., Chambouvet, A., Florent, I., Guillou, L., 2016. Ultrastructure of *Selenidium pendula*, the Type Species of Archigregarines, and Phylogenetic Relations to Other Marine Apicomplexa. Protist 167, 339–368. https://doi.org/10.1016/j.protis.2016.06.001.

Simdyanov, T.G., Guillou, L., Diakin, A.Y., Mikhailov, K.V., Schrével, J., Aleoshin, V.V., 2017. A new view on the morphology and phylogeny of eugregarines suggested by the evidence from the gregarine *Ancora sagittata* (Leuckart, 1860) Labbé, 1899 (Apicomplexa: Eugregarinida). PeerJ 5, 1–46. https://doi.org/10.7717/peerj.3354.

Sitnikova, T.Y., Shirokaya, A.A., 2013. New data in deep-water Baikal limpets found in hydrothermal vents and oil-seeps. Arch. für Molluskenkd. 142, 257–278. https://doi.org/10.1127/arch.moll/1869-0963/142/257-278.

Stach, T., Turbeville, J.M., 2002. Phylogeny of Tunicata inferred from molecular and morphological characters. Mol. Phylogenet. Evol. 25, 408–428. https://doi.org/10.1016/S1055-7903(02)00305-6.

Stamatakis, A., 2014. RAxML version 8: A tool for phylogenetic analysis and post-analysis of large phylogenies. Bioinformatics 30, 1312–1313. https://doi.org/10.1093/bioinformatics/btu033.

Théodoridès, J., 1967. Sur la position systématique du genre *Lankesteria* Mingazzini, 1891 (Eugregarina). CR Acad Sci Hebd Seances Acad Sci D 265, 1995–1996.

Turon, X., López-Legentil, S., 2004. Ascidian molecular phylogeny inferred from mtDNA data with emphasis on the Aplousobranchiata. Mol. Phylogenet. Evol. 33, 309–320. https://doi.org/10.1016/j.ympev.2004.06.011.

Wakeman, K.C., Leander, B.S., 2013. Identity of environmental DNA sequences using descriptions of four novel marine gregarine parasites, *Polyplicarium* n. gen. (Apicomplexa), from capitellid polychaetes. Mar. Biodivers. 43, 133–147. https://doi.org/10.1007/s12526-012-0140-5.

Wakeman, K.C., Leander, B.S., 2012. Molecular phylogeny of pacific archigregarines (Apicomplexa), including descriptions of *Veloxidium leptosynaptae* n. gen., n. sp., from the sea cucumber *Leptosynapta clarki* (Echinodermata), and two new species of *Selenidium*. J. Eukaryot. Microbiol. 59, 232–245. https://doi.org/10.1111/j.1550-7408.2012.00616.x.

Wilson, (Iain) R.J.M., Denny, P.W., Preiser, P.R., Rangachari, K., Roberts, K., Roy, A., Whyte, A., Strath, M., Moore, D.J., Moore, P.W., Williamson, D.H., 1996. Complete Gene Map of the Plastid-like DNA of the Malaria Parasite Plasmodium falciparum. J. Mol. Biol. 261. https://doi.org/10.1006/jmbi.1996.0449.

World Health Organization., 2018. World malaria report 2018. World Heal. Organ. 1–166.

Yamaguchi, A., Kawamura, H., Horiguchi, T., 2005. A further phylogenetic study of the heterotrophic dinoflagellate genus , Protoperidinium (Dinophyceae) based on small and large subunit ribosomal RNA gene sequences 317–329.

Zhan, A., Briski, E., Bock, D.G., Ghabooli, S., MacIsaac, H.J., 2015. Ascidians as models for studying invasion success. Mar. Biol. 162, 2449–2470. https://doi.org/10.1007/s00227-015-2734-5.

Zuk, M., 1987. The effects of gregarine parasites on longevity, weight loss, fecundity and developmental time in the field crickets *Gryllus veletis* and *G. pennsylvanicus*. Ecol. Entomol. 12, 349–354. https://doi.org/10.1111/j.1365-2311.1987.tb01014.x.